Asian Spine Journal
Clinical Study
Asian Spine J 2024;18(1):110-117 • https://doi.org/10.31616/asj.2023.0234

# Establishment of the Lunar Phase Morphological Classification for Cervical Spinal Canal

Zhongyi Cui[1,*], Hongwei Wang[2,*], Yuan Sun[3,*], Weibo Huang[2], Fei Zou[2], Xiaosheng Ma[2], Feizhou Lyu[1,2], Jianyuan Jiang[2], Hongli Wang[2]

[1]*Department of Orthopaedics, Shanghai Fifth People's Hospital, Fudan University, Shanghai, China*
[2]*Department of Orthopaedics, Huashan Hospital, Fudan University, Shanghai, China*
[3]*Department of Nursing, Huashan Hospital, Fudan University, Shanghai, China*

**Study Design:** Retrospective clinical trial.

**Purpose:** To establish a morphological classification of the cervical spinal canal using its parameters.

**Overview of Literature:** Cervical spine computed tomography (CT) data of 200 healthy volunteers in 2 years were analyzed. The morphology of the spinal cord was also analyzed.

**Methods:** The median sagittal diameter and transverse diameter of the spinal canal from C2 to C7 were measured on CT images. The ratio of the median sagittal diameter to the transverse diameter was calculated. Accordingly, the spinal canal shape of each segment was classified into four, and the specific criteria of lunar phase classification were determined through linear discriminant analysis based on the ratio of the median sagittal diameter to the transverse diameter. The inter-rater reliability of the classification was explored using Kappa coefficients. Finally, the morphology of the different segments of the cervical spinal canal in healthy volunteers was revised and compared.

**Results:** According to the ratio of the median sagittal diameter and the transverse diameter of the cervical spinal canal, the lunar phase classification of the cervical bony spinal canal was determined as follows: full-moon >0.65, 0.55< convex-moon ≤0.65, 0.46≤ quarter-moon ≤0.55, and residual-moon <0.46. The Kappa values of C2–C7 were 0.851, 0.958, 0.823, 0.927, 0.793, and 0.946, and the Kappa value of all C2–C7 segments was 0.854 that mainly presented two forms of full-moon (76.5%) and convex-moon (23.0%). A quarter-moon spinal canal was mainly distributed in C3, C4, C5, and C6; a residual-moon spinal canal was mainly distributed in C4 and C5; and the morphological distribution of C4 and C5 were similar ($p$>0.05). The frequency of the spinal canal of the residual-moon type was the highest, and the full-moon (6.5%) and residual-moon (7.5%) types of C7 were rare.

**Conclusions:** The morphological classification of the cervical spinal canal was established to present anatomical variations. The classification showed good inter-rater reliability.

**Keywords:** Cervical vertebrae; Cervical spondylotic myelopathy; Bony spinal canal; Classification

Received Jul 11, 2023; Revised Aug 13, 2023; Accepted Sep 18, 2023

Corresponding author: Hongli Wang
Department of Orthopaedics, Huashan Hospital, Fudan University, No. 12 Middle Wulumuqi Road, Shanghai, 200040 China
Tel: +86-21-52887274, Fax: +86-21-52887274, E-mail: wanghongli0212@163.com; wanghongli@huashan.org.cn
Co-corresponding author: Jianyuan Jiang
Department of Orthopaedics, Huashan Hospital, Fudan University, No. 12 Middle Wulumuqi Road, Shanghai, 200040 China
Tel: +86-21-52887274, Fax: +86-21-52887274, E-mail: jjy@fudanspine.com
*These authors contributed equally to this work as the first authors.

## Introduction

Cervical spinal stenosis is an important pathogenesis of cervical spondylotic myelopathy. For patients with developmental spinal stenosis, the spinal cord is more susceptibly compressed by osteophytes and intervertebral discs. Thus, the cervical spinal canal must be effectively evaluated for the early risk assessment of cervical spondylosis and the identification of appropriate surgical techniques.

Nowadays, the Pavlov ratio is a world-recognized tool to measure and evaluate cervical spinal stenosis. In 1986, Torg et al. [1] proposed the cervical spinal canal ratio (also known as Pavlov ratio); this is the ratio of the sagittal diameter of the spinal canal to the median sagittal diameter (MSD) of the vertebral body to eliminate the influence of the magnification of the X-ray lateral view. Pavlov et al. [2] further examined this and suggested that cervical spinal canal stenosis could be diagnosed if the Pavlov ratio was <0.82. However, the Pavlov ratio has limitations. First, it cannot exclude the influence of vertebral body variations. Second, it ignores the transverse diameter (TD) of the spinal canal. Thus, many researchers believe that the Pavlov ratio may not truly reflect the size of the spinal canal [3,4].

How to accurately and effectively evaluate the morphology of the cervical spinal canal is now a controversial topic. Some researchers have sought to assess the shape of the spinal canal shape based on the cross-sectional area of the spinal canal or multiple parameters including lateral masses, lamina lengths, and lamina–pedicle angles. However, these measurement studies have shortcomings such as limited ability in decreasing the influence based on individual variations and requiring extracomplicated procedures [5-9]. A simpler method with acceptable accuracy is yet to be explored.

However, based on lumbar computed tomography (CT), Meyer has established a morphological classification of the lumbar spinal canal, including the round, oval, and trefoil shapes. Choi et al. [10] found that microsurgical bilateral decompression via a unilateral approach was less effective in trefoil-shaped spinal canal stenosis, proving the clinical application value of Myer's classification. Inspired by Meyer's classification of the lumbar spinal canal, we assumed that a similar classification could be initiatively established to assess the morphology of the cervical spinal canal.

Therefore, this study aimed to establish the classification system based on the relationship between the sagittal diameter and the TD of the spinal canal and to test its reliability. Meanwhile, the morphological differences of each segment of the cervical spine were compared to provide a theoretical basis for the potential risk of cervical spinal cord compression in patients with cervical spinal stenosis.

## Materials and Methods

### 1. Inclusion and exclusion criteria for healthy volunteers

This study was approved by the ethical committee of the authors' hospital. The requirement for informed consent from individual patients was omitted because of the retrospective design of this study. Asymptomatic adults who underwent imaging between January 2018 and December 2019 were included. Individuals with a history of (1) craniocerebral and cervical spine trauma, (2) cervical spondylosis, ossification of the posterior longitudinal ligament of the cervical spine, (3) cervical spine deformity, (4) intraspinal space occupation and neurological diseases, and (5) history of cervical spine surgery or any other history that may affect the measurement were excluded. Following the inclusion and exclusion criteria, 200 healthy volunteers were included, including 124 men and 76 women. The average age was 52.39±10.01 years.

### 2. Computed tomography equipment and methods

Cervical CT images were obtained with a 256-slice spiral CT scanner (Ingenuity TF CT; Philips, Amsterdam, Netherlands) with a tube voltage of 100 kV and a current of 331 mA. The slice thickness was 1.5 mm with a slice gap of 1.5 mm. The patient takes the supine position. Images were processed with Philips IntelliSpace Portal (philips.com) by applying two-dimensional reconstruction when the scans were completed.

### 3. Measurement of related parameters of the spinal canal and classification of the spinal canal morphology

1) Measurement of cervical spinal canal parameters
The slices of the transverse axial section of the cervical spine crossing the midpoint of the posterior edge of the vertebral body were acquired with Philips IntelliSpace Portal at different segments. As shown in Fig. 1, the MSD and TD of the bony spinal canal were measured. The MSD was measured between the midpoint of the anterior wall

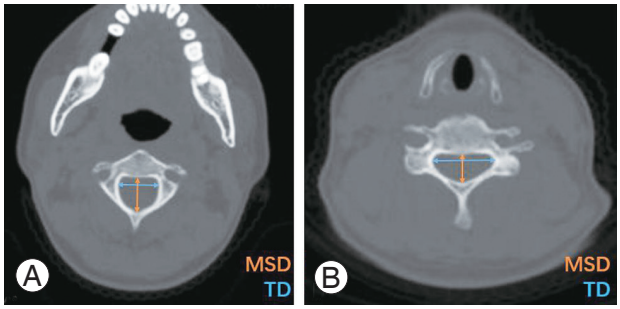


**Fig. 1.** The measurements of median sagittal diameter (MSD) and transverse diameter (TD) of the spinal canal on computed tomography images. **(A)** C2 segment measurement. **(B)** C3–7 segments measurment.

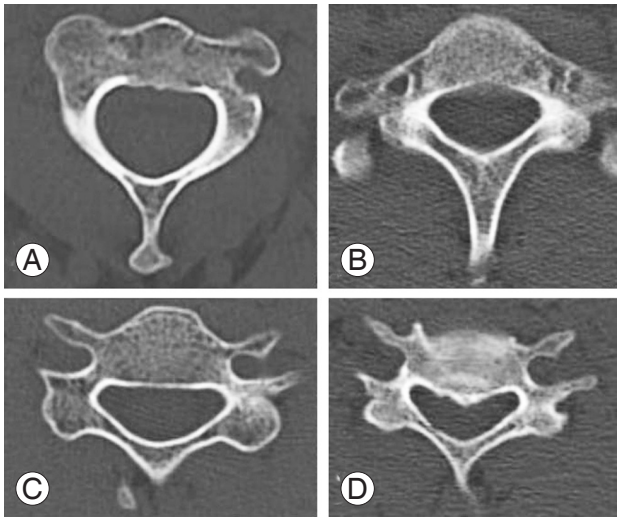


**Fig. 2.** The four morphological types of cervical spinal canal. **(A)** Full moon type. **(B)** Convex moon type. **(C)** Quarter moon type. **(D)** Residual moon type.

and the posterior wall of the bony spinal canal. TD is the distance between the two lateral points of the spinal canal. At C2, the MSD and TD were measured at the level 1 cm downward from the C2 inferior endplate and parallel to the level of the C2 inferior endplate. The measurements were accomplished by two spine surgeons (Z.C. and HW. W.), and the results were averaged and recorded.

2) Morphological records of the cervical spinal canal
In our initial observation of the morphology of C2–C7, the morphology of each segment of the cervical spine also had a certain evolutionary form. To describe the shape of the spinal canal, the concept of lunar phases was introduced herein. As presented in Fig. 2, given that the shapes of the spinal canal have certain similarities with the phases of the moon, we classified the morphology of the cervical spinal canal into four main types, namely, full-moon, convex-moon, quarter-moon, and residual-moon based on the similarity.

When measuring the MSD and TD, two experienced spine surgeons (F.Z. and HL. W.) observed and recorded the morphology of different cervical segments. When the recorded spinal canal morphology differed between them, the third senior surgeon (X.M.) was invited to observe and determine the morphology of the spinal canal.

### 4 Establishment of the lunar phase classification of the cervical spinal canal

Then, the ratio of the MSD to the TD of each segment was calculated, and linear discriminant analysis with the morphology of each segment was performed to quantify the morphological classification of the bony spinal canal. According to the classification criterion, the morphology of each segment of the bony spinal canal was reclassified.

### 5. Reliability verification of the lunar phase classification

After the classification was established, two additional surgeons (F.L. and J.J.) were invited to learn and use the lunar phase classification. To verify the reliability, these two experienced surgeons (F.L. and J.J.) conducted morphological classification of each segment in 30 additional volunteers.

### 6. Statistical analysis

Statistical analysis was performed with IBM SPSS Statistics ver. 22.0 (IBM Corp., Armonk, NY, USA). Measurement data are expressed as mean±standard deviation for continuous data and percentage for noncontinuous data. Linear discriminant analysis was performed to quantify the classification of the cervical spinal canal. Kappa values were used to test the consistency of the classification. The chi-square test was used to compare whether the morphological distribution of the different segments of the spinal canal was different.

## Results

### 1 Measurement results of cervical vertebral canal parameters

The MSD and TD results of the cervical spinal canal at

**Table 1.** The median sagittal diameter and transverse diameter of each segment

| | MSD (mm) | TD (mm) |
|---|---|---|
| C2 | 15.51±1.43 | 22.74±1.97 |
| C3 | 11.79±1.53 | 22.50±2.13 |
| C4 | 11.27±1.46 | 23.74±2.37 |
| C5 | 11.52±1.48 | 24.28±2.50 |
| C6 | 12.08±1.95 | 23.97±2.59 |
| C7 | 12.77±1.88 | 22.84±2.42 |

Values are presented as mean±standard deviation.
MSD, median sagittal diameter; TD, transverse diameter.

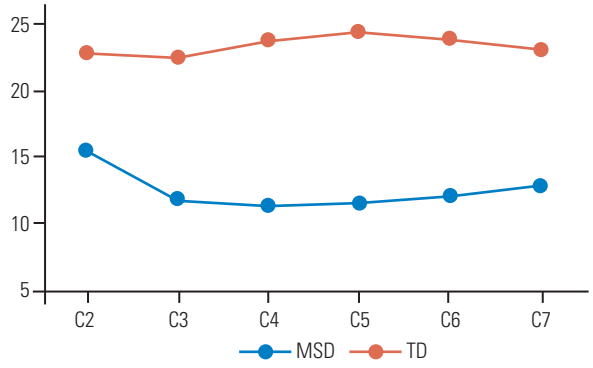


**Fig. 3.** The changing trend of median sagittal diameter (MSD) and transverse diameter (TD) of the cervical spinal cord.

each segment of the cervical spine of healthy volunteers are shown in Table 1. The MSD of the spinal canal of the C2–C7 segment gradually decreases from C2 to C4 and then gradually increases from C4 to C7. TD showed a trend of gradually increasing from C2 to C5 and then gradually decreasing from C5 to C7 (Fig. 3).

### 2 Quantify the morphological classification of the cervical spinal canal

Through the linear discriminant analysis, with the spinal canal MSD and TD as independent variables and spinal canal morphology as the dependent variable, the established spinal canal morphology discriminant function is as follows: full-moon-type spinal canal, Y1=716.211X1–254.386; convex-moon-type spinal canal, Y2=600.799X2–179.418; quarter-moon-type spinal canal, Y3=505.24X3–127.288; and residual-moon-type spinal canal, Y4=426.71X4–91.192. According to the linear discriminant analysis, the independent variable was substituted into each discriminant function, which was the largest dependent variable that could distinguish its shape.

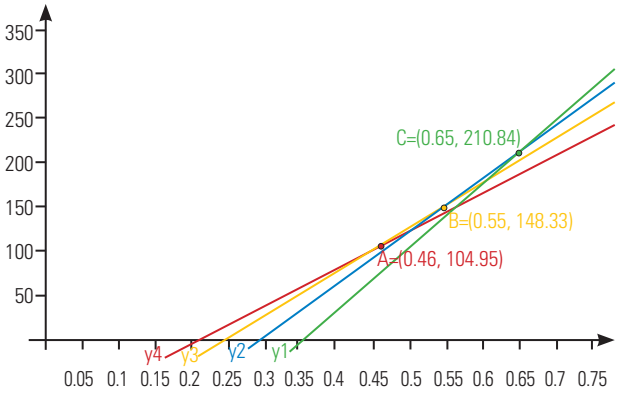


**Fig. 4.** Discrimination function of the lunar phase classification.

**Table 2.** The Kappa value and 95% CI of each segment

| Segment | Kappa (95% CI) |
|---|---|
| C2 | 0.851 (0.653–1.048) |
| C3 | 0.958 (0.877–1.039) |
| C4 | 0.823 (0.630–1.015) |
| C5 | 0.927 (0.786–1.067) |
| C6 | 0.793 (0.604–0.982) |
| C7 | 0.946 (0.844–1.048) |
| C2–C7 | 0.854 (0.800–0.907) |

CI, confidence interval.

Therefore, the intersection points for morphological discrimination are A (0.46, 104.95), B (0.55, 148.33), and C (0.65, 210.84). The image of each discriminant function and the intersection point of morphological discrimination are shown in Fig. 4. The established discriminant function finally correctly classified 92.8% of the observed patterns.

Therefore, according to the ratio of the MSD to the TD of the spinal canal, the lunar phase classification of the cervical spinal canal is quantified as follows: full-moon type >0.65, 0.55< convex-moon type ≤0.65, 0.46≤ quarter-moon type ≤0.55, and residual-moon type <0.46.

### 3. Reliability verification of lunar phase typing

The Kappa values of each segment from C2 to C7 were 0.851, 0.958, 0.823, 0.927, 0.793, and 0.946, respectively, and the Kappa value of all C2–C7 segments was 0.854. The cervical spinal canal lunar phase classification was

consistent between the two observers, and the application of the lunar phase classification was reliable (Table 2).

### 4. Reclassification of the spinal canal morphology

According to the quantitative classification criteria, the final spinal canal morphology of each segment of the healthy volunteers was as follows: C2, 153 cases of full-moon type, 46 of convex-moon type, and one of quarter-moon type; C3, four of full-moon type, 50 cases of convex-moon type, 121 of quarter-moon type, and 25 of residual-moon type; C4, one case of full-moon type, 14 of convex-moon type, 110 of quarter-moon type, and 75 of residual-moon type; C5, 14 of convex-moon type, 102 of quarter-moon type, and 84 of residual-moon type; C6, three cases of full-moon type, 47 of convex-moon type, 96 of quarter-moon type, and 54 of residual-moon type; C7, 13 cases of full-moon type, 104 of convex-moon type, 68 of quarter-moon type, and 15 of residual-moon type (Fig. 5).

### 5 Comparison of the morphological distribution of each segment

The morphological distribution of the spinal canal of each

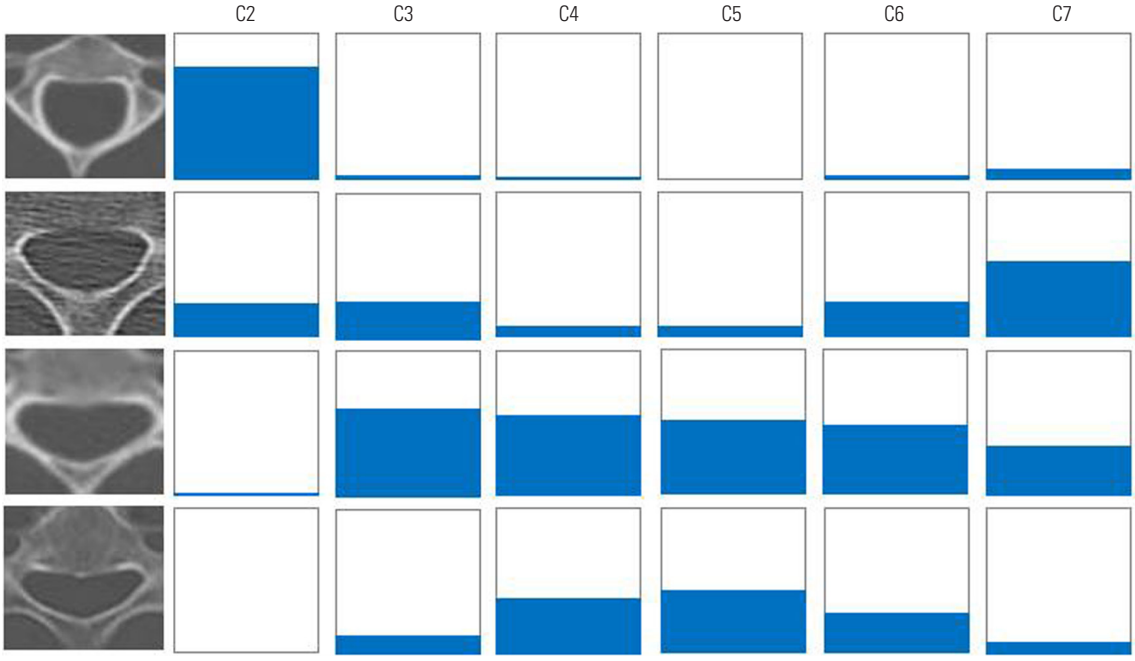


**Fig. 5.** The morphological distribution of each segment.

**Table 3.** Crosstabulation of morphological type and cervical segment[a]

| Morphological type | Category | Segment | | | | | |
|---|---|---|---|---|---|---|---|
| | | C2 | C3 | C4 | C5 | C6 | C7 |
| Full moon type | Frequencies | 153 | 4 | 1 | 0 | 3 | 13 |
| | Adjusted residual | (27.3) | (-5.5) | (-6.2) | (-6.4) | (-5.7) | (-3.5) |
| Convex moon type | Frequencies | 46 | 50 | 14 | 14 | 47 | 104 |
| | Adjusted residual | (0) | (0.8) | (-5.9) | (-5.9) | (0.2) | (10.7) |
| Quarter moon type | Frequencies | 1 | 121 | 110 | 102 | 96 | 68 |
| | Adjusted residual | (-12.9) | (6.0) | (4.2) | (3.0) | (2.0) | (-2.4) |
| Residual moon type | Frequencies | 0 | 25 | 75 | 84 | 54 | 15 |
| | Adjusted residual | (-8.0) | (-3.3) | (6.2) | (7.9) | (2.2) | (-5.2) |

[a]Adjusted residual appear in parentheses below observed frequencies.

segment was compared and was significantly different ($\chi^2$=1,011.715, $p$<0.001). The morphological distribution was associated with the cervical segment (Creamer's V=0.530, $p$<0.001). The morphological distribution of C2, C3, and C7 consisted of spinal canal shapes with larger MSD; meanwhile, the morphological distribution of C4 and C5 consisted of shapes with smaller MSD. The post hoc testing results are shown in Table 3.

## Discussion

### 1 Establishment and reliability verification of the lunar phase classification

The morphology of the spinal canal has been ignored in previous imaging measurement studies; however, anatomical studies have proved that morphological differences exist in the cervical spinal canal segments. Chazono et al. [11] found that the overall anterior–posterior diameter of the spinal canal was higher in Europeans/Americans than in Asians. The potential clinical application value of cervical spinal canal morphological classification has been ignored. The measurement results of the spinal canal parameters showed that the sagittal diameter of the cervical spine is smaller than the TD, the TD of the C2–C7 spinal canal first increased and then decreased, and the sagittal diameter first decreased and then increased. This is highly consistent with the conclusions of the anatomical research. Owing to the relationship between the sagittal diameter and TD, we cannot establish the classification just as the Meyer classification [10]. Therefore, the ratio between the parameters was calculated, and the sagittal median diameter/TD showed a certain correlation with the spinal canal shape. Furthermore, the lunar phase classification standard was as follows: full-moon type >0.65, 0.55< convex-moon type ≤0.65, 0.46≤ quarter-moon type ≤0.55, and residual-moon type <0.46 through the linear discriminant analysis. In the reliability verification, the Kappa coefficients of each segment were 0.851, 0.958, 0.823, 0.927, 0.793, and 0.946, whereas the Kappa coefficient of C2–C7 was 0.854, which was greater than 0.81, confirming the reliability of the lunar phase classification.

### 2 Comparison of the morphological distribution of the spinal canal segments

After the classification was established, we reclassified the morphology of each segment according to the classification criteria, which further confirmed the difference in the morphological distribution of each segment of the cervical spine. The C2 segment is dominated by the full-moon (76.5%) and convex-moon (23%) types with a larger sagittal diameter. This is also consistent with less spinal cord compression in C2 because C2 has a larger sagittal diameter to accommodate the spinal cord. The main type of the spinal canals in C3–C6 was the quarter-moon type, which account for 60.5%, 55%, 51%, and 48% of all segments. The most common type in C7 was the convex-moon type (52%). Starting from C3, the residual-moon type with a smaller sagittal diameter begins to appear, and C4–C6 account for 37.5%, 42%, and 27% of their respective segments, which makes it possible to compress the cervical spinal cord in this segment. The convex-moon type is the main type of C7, which has a larger space to accommodate the spinal cord.

Many studies have shown that C5/6 is the segment with the most surgical interventions available for cervical spondylotic myelopathy [12-14]. C5 had a more residual-moon-type canal with the smallest sagittal diameter. The electrophysiological study by Tani et al. [15] found that the C3/4 and C4/5 of their patients aged >65 years accounted for 95% of the total. It appears different from the usual surgical intervention segment. Tani et al. [15] explained that with growing age, osteophytes proliferate, C5/6 range of motion (ROM) decreases, C3/4 and C4/5 ROM increases, and it is more likely to have spinal cord compression injury. Electrophysiological examination is normally called asymptomatic compression or "silent spinal cord compression [15]." In the comparison of the morphological distribution of the spinal canals, we can find that C3–C6 has a more residual-moon type of the spinal canal, and the proportion of C4 and C5 residual-moon type of the spinal canal is higher than that of C6. Perhaps this difference can explain the question above. The risk of spinal cord compression increased with the sagittal diameter getting smaller. The proportion of the residual-moon-type spinal canal in C4 and C5 is higher than that in other segments. Therefore, compression or motion is more likely to cause cervical spinal cord injury.

### 3. Interpretation of the lunar phase classification

The size of the vertebral body as a risk factor for CSM is controversial. Hukuda et al. [16] suggested that a large

vertebral body is a risk factor for cervical myelopathy. However, Lu et al. [17] found that smaller vertebral bodies are an attributing factor of cervical spondylosis. Prasad et al. [18] also proved that the Pavlov ratio poorly correlated with the space for the spinal cord. Meanwhile, congenital spinal stenosis is a risk factor of CSM [19], which means that the diameter of the spinal canal cannot be ignored to evaluate patients with CSM. Different from the Pavlov ratio, the lunar phase classification only uses spinal canal parameters for quantification and does not mix other parameters. Therefore, it can more realistically reflect the volume of the spinal canal.

In the morphological classification of the cervical spinal canal, the sagittal diameter of the spinal canal of the quarter-moon and residual-moon types is smaller than that of the full-moon and convex-moon types. As known, cervical spinal stenosis is an important pathogenesis of cervical spondylotic myelopathy. The type of spinal canal can just reflect the decreasing sagittal diameter. Thus, the last two types are related to cervical spondylotic myelopathy; however, further studies are needed to prove it.

## Conclusions

This study initially establishes the lunar phase classification of the cervical spinal canal, and the classification is reliable. The quarter- and residual-moon types of spinal canals may be related to cervical spondylotic myelopathy.

## Conflict of Interest

No potential conflict of interest relevant to this article was reported.

## ORCID

Zhongyi Cui: https://orcid.org/0000-0002-2415-3453; Hongwei Wang: https://orcid.org/0000-0002-9497-7650; Yuan Sun: https://orcid.org/0009-0007-6923-9676; Weibo Huang: https://orcid.org/0000-0002-9005-0401; Fei Zou: https://orcid.org/0000-0002-8088-6045; Xiaosheng Ma: https://orcid.org/0000-0001-5882-1651; Feizhou Lyu: https://orcid.org/0000-0003-2431-0591; Jianyuan Jiang: https://orcid.org/0009-0009-0191-1387; Hongli Wang: https://orcid.org/0000-0002-2096-6625

## Author Contributions

Conceptualization: ZC, Hongli W; data curation: Hongwei W, WH; formal analysis: ZC; funding acquisition: JJ, Hongli W; methodology: ZC, Hongwei W, WH; visualization: FZ, XM, FL, JJ, Hongli W; writing–originial draft: ZC, HW, YS; writing–review & editing: FZ, XM, FL, JJ, Hongli W; and final approval of the manuscript: all authors.

## References

1. Torg JS, Pavlov H, Genuario SE, et al. Neurapraxia of the cervical spinal cord with transient quadriplegia. J Bone Joint Surg Am 1986;68:1354-70.
2. Pavlov H, Torg JS, Robie B, Jahre C. Cervical spinal stenosis: determination with vertebral body ratio method. Radiology 1987;164:771-5.
3. Portillo-Portillo J, Leyva R, Sanchez V, et al. Cross view gait recognition using joint-direct linear discriminant analysis. Sensors (Basel) 2016;17:6.
4. Kanai R, Ohshima K, Ishii K, et al. Discriminant analysis and interpretation of nuclear chromatin distribution and coarseness using gray-level co-occurrence matrix features for lobular endocervical glandular hyperplasia. Diagn Cytopathol 2020;48:724-35.
5. Tierney RT, Maldjian C, Mattacola CG, Straub SJ, Sitler MR. Cervical spine stenosis measures in normal subjects. J Athl Train 2002;37:190-3.
6. Matveeva N, Janevski P, Nakeva N, Zhivadinovik J, Dodevski A. Morphometric analysis of the cervical spinal canal on MRI. Pril (Makedon Akad Nauk Umet Odd Med Nauki) 2013;34:97-103.
7. Nell C, Bulow R, Hosten N, Schmidt CO, Hegenscheid K. Reference values for the cervical spinal canal and the vertebral bodies by MRI in a general population. PLoS One 2019;14:e0222682.
8. Nouri A, Montejo J, Sun X, et al. Cervical cord-canal mismatch: a new method for identifying predisposition to spinal cord injury. World Neurosurg 2017;108:112-7.
9. Jenkins TJ, Mai HT, Burgmeier RJ, Savage JW, Patel AA, Hsu WK. The triangle model of congenital cervical stenosis. Spine (Phila Pa 1976) 2016;41:E242-7.
10. Choi WS, Oh CH, Ji GY, et al. Spinal canal morphology and clinical outcomes of microsurgical bilateral decompression via a unilateral approach for lumbar

spinal canal stenosis. Eur Spine J 2014;23:991-8.
11. Chazono M, Tanaka T, Kumagae Y, Sai T, Marumo K. Ethnic differences in pedicle and bony spinal canal dimensions calculated from computed tomography of the cervical spine: a review of the English-language literature. Eur Spine J 2012;21:1451-8.
12. Hayashi H, Okada K, Hamada M, Tada K, Ueno R. Etiologic factors of myelopathy: a radiographic evaluation of the aging changes in the cervical spine. Clin Orthop Relat Res 1987;(214):200-9.
13. Wu W, Thuomas KA, Hedlund R, Leszniewski W, Vavruch L. Fast spin-echo MR assessment of patients with poor outcome following spinal cervical surgery. Acta Radiol 1996;37:153-61.
14. Arnold H, Feldmann U, Missler U. Chronic spondylogenic cervical myelopathy: a critical evaluation of surgical treatment after early and long-term follow-up. Neurosurg Rev 1993;16:105-9.
15. Tani T, Yamamoto H, Kimura J. Cervical spondylotic myelopathy in elderly people: a high incidence of conduction block at C3-4 or C4-5. J Neurol Neurosurg Psychiatry 1999;66:456-64.
16. Hukuda S, Xiang LF, Imai S, Katsuura A, Imanaka T. Large vertebral body, in addition to narrow spinal canal, are risk factors for cervical myelopathy. J Spinal Disord 1996;9:177-86.
17. Lu X, Tian Y, Wang SJ, et al. Relationship between the small cervical vertebral body and the morbidity of cervical spondylosis. Medicine (Baltimore) 2017;96:e7557.
18. Prasad SS, O'Malley M, Caplan M, Shackleford IM, Pydisetty RK. MRI measurements of the cervical spine and their correlation to Pavlov's ratio. Spine (Phila Pa 1976) 2003;28:1263-8.
19. Nouri A, Tetreault L, Singh A, Karadimas SK, Fehlings MG. Degenerative cervical myelopathy: epidemiology, genetics, and pathogenesis. Spine (Phila Pa 1976) 2015;40:E675-93.